International Journal of Innovative
Computing, Information and Control
Volume **19**, Number **5**, October **2023**

ICIC International ©2023 ISSN 1349-4198
pp. **1425–1437**

MAXIMUM POWER POINT TRACKING CONTROL FOR PHOTOVOLTAIC SYSTEMS USING MODIFIED BAYESIAN OPTIMIZATION

Eiji Masuda[1], Yasuki Sogawa[2], Yuji Wakasa[3] and Ryosuke Adachi[3]

[1]Yamaguchi Prefectural Industrial Technology Institute
4-1-1 Asutopia, Ube, Yamaguchi 755-0195, Japan
masuda@iti-yamaguchi.or.jp

[2]Chudenko Corporation
6-12 Koamicho, Naka-ku, Hiroshima 730-0855, Japan
y.sogawa@chudenko.co.jp

[3]Graduate School of Sciences and Technology for Innovation
Yamaguchi University
2-16-1 Tokiwadai, Ube, Yamaguchi 755-8611, Japan
{ wakasa; r-adachi }@yamaguchi-u.ac.jp

Received January 2023; revised May 2023

Abstract. *In photovoltaic (PV) systems, a maximum power point tracking (MPPT) controller is essential for optimizing the PV output. The controller must be able to find the global maximum power point (MPP) fast even when the power-voltage curve has multiple local MPPs. This paper presents a modified Bayesian optimization (BO) algorithm and applies it to MPPT control for PV systems. By using the Lipschitz continuity of the objective function, the presented algorithm reduces unnecessary exploration and accelerates the convergence of the standard BO algorithm. In numerical simulation, we compare the presented algorithm with some MPPT methods and validate its effectiveness in terms of convergence time and power loss.*

Keywords: Maximum power point tracking control, Partial shading condition, Bayesian optimization, Lipschitz continuity

1. **Introduction.** To break our dependence on fossil fuels, the effective use of renewable energy sources has been desired. Notably, photovoltaic (PV) generation has been spreading all over the world because of its practicality and efficiency.

The power-voltage (P-V) curves of a PV array vary with weather conditions such as panel temperature and solar radiation. A maximum power point tracking (MPPT) controller is a crucial component for obtaining the maximum power point (MPP) in response to the weather changes. MPPT control algorithms aim to find the MPP without weather observation devices. As a result, an MPPT control problem can be characterized as a black-box optimization problem.

A major challenge of the MPPT control problem is to find the global MPP even if the P-V curves have multiple local MPPs under partial shading conditions. In these conditions, typical MPPT methods, such as the hill climbing (HC) [1] and incremental conductance methods [2, 3], may find a local MPP. More recently, the fuzzy state-feedback control-based MPPT method has been presented in [4]. This method is robust for climate change and saves the oscillation near the MPP; however, this method may also find a local MPP. To cope with this issue, scanning-based and metaheuristics-based MPPT methods, such

DOI: 10.24507/ijicic.19.05.1425

as window-scanning method [5], grey wolf optimization [6], Jaya algorithm [7, 8], and salp swarm optimization [9], have been presented. These methods can find the global MPP reliably (or with a high probability); however, these methods are somewhat inefficient because the methods tend to excessively search the domain of the objective function.

In contrast to the abovementioned local and stochastic MPPT methods, a Lipschitz optimization (LO)-based MPPT algorithm has been presented [10]. LO is guaranteed to deterministically converge to the global optimum of a function satisfying the Lipschitz continuity over a closed set [11, 12]. LO iteratively evaluates the objective function value and estimates an upper bound of the objective function based on the Lipschitz condition. As the algorithm proceeds, the upper bound decreases, and the candidate regions containing the global optimal solution are simultaneously restricted. In [13, 14], accelerated LO algorithms using the prior information on the objective function value have been proposed and applied to the MPPT control problem. However, LO-based MPPT methods as well as general deterministic algorithms tend to excessively search the domain of the objective function and evaluate too many low power points. Consequently, these MPPT methods cause low MPPT efficiency, i.e., power loss.

Meanwhile, Bayesian optimization (BO) has been implemented in the MPPT control problem [15]. BO is global optimization based on a stochastic process and finds the optimum of a black-box function or an expensive-to-evaluate function. In particular, BO has been successful at hyper-parameter tuning in machine learning recently. However, BO tends to explore excessively the search space to find the global MPP.

In this paper, we present modified BO (MBO) which utilizes the Lipschitz continuity of the objective function and apply it to the MPPT control problem. The Lipschitz continuous function is limited in its gradient to a bounded constant. By using this property, the existence region of the global optimal solution is restricted. As a result, the convergence of BO can be accelerated. In the application of MBO to the MPPT control problem, finding the global MPP is much more efficient than continuing to track a local MPP in terms of the economical use of solar energy. Additionally, a more efficient use of solar energy can be achieved by finding the global MPP faster. We build a simulation model of the PV system using MATLAB/Simulink. The LO [10] and BO [15]-based MPPT methods, which are global optimization methods and show the good performance, are opted to compare with the presented method.

The remainder of this paper is organized as follows. The MPPT control problem is described in Section 2. Some mathematical preliminaries and the BO algorithm are explained in Section 3. In Section 4, we present MBO for the MPPT control problem. Section 5 gives simulation results to validate its effectiveness. In the final section, the conclusion of this paper is given.

2. MPPT Control Problem.

The simple PV system diagram is illustrated in Figure 1. In Figure 1, I_{PV} and V_{PV} are the output current and output voltage, respectively, of the PV panel. The role of the MPPT controller is to maximize the output of the PV array by modulating the duty cycle of the DC-DC converter. In this section, the characteristics of the PV array and the DC-DC converter are described.

2.1. Characteristics of PV array.

Figure 2 depicts the current-voltage (I-V) and power-voltage (P-V) curves of the PV array and the load line, where $P_{\mathrm{PV}} = I_{\mathrm{PV}}V_{\mathrm{PV}}$. In Figure 2, I_{MPP} and V_{MPP} are the current and voltage, respectively, for the MPP. The operating point of the PV array is given by the intersection of the I-V curve and the load line. The area of the square implies the maximum output power. The slope of the load

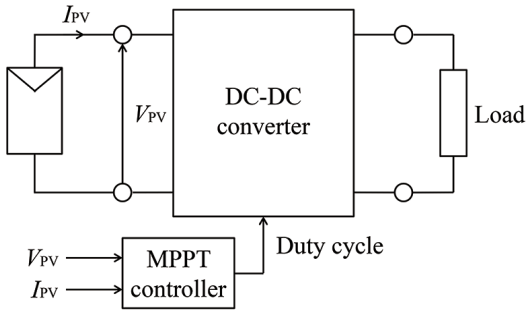

FIGURE 1. PV system

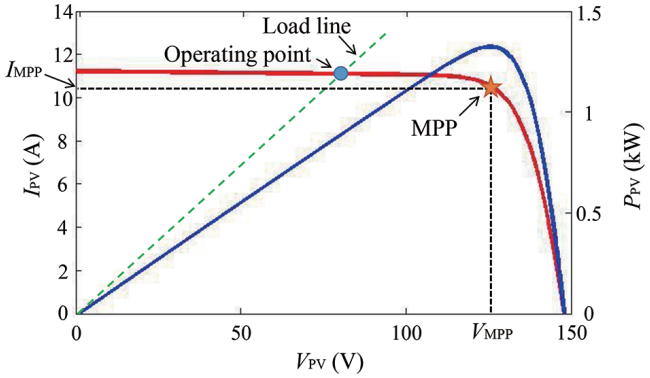

FIGURE 2. I-V and P-V curves of PV array and load line

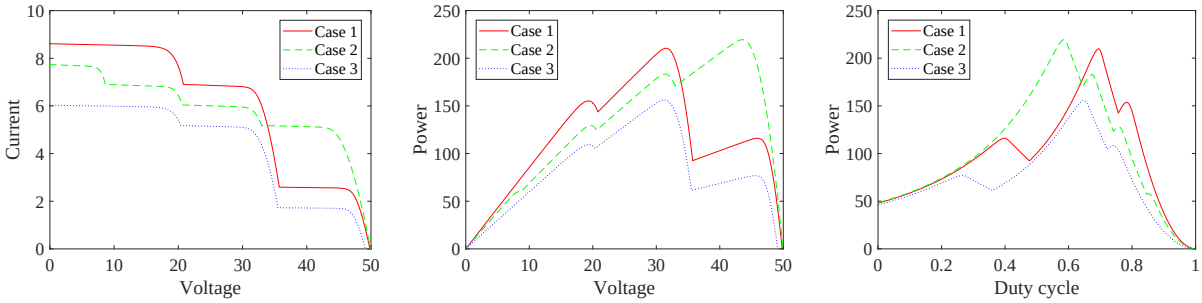

(a) I-V characteristics (b) P-V characteristics (c) P-D characteristics

FIGURE 3. Characteristics of PV array under partial shading conditions

line depends on the load magnitude. The MPPT controller aims to match the operating point and the MPP by controlling the slope of the load line.

Under a uniform solar irradiance condition, the I-V curve exhibits a single step, as shown in Figure 2. In contrast, under nonuniform solar irradiance conditions due to partial shading situations, the I-V curves exhibit multiple steps, as shown in Figure 3(a). Then, the corresponding P-V curves have multiple local MPPs, as shown in Figure 3(b). Note that, in Figure 3, we simulate the PV panel characteristics under three different partial shading cases by connecting four PV panels with different output power, as described later in Subsection 5.1.

2.2. **DC-DC converter.** Figure 4 illustrates a boost converter, where L is inductance, C is capacitance, V_C is the output voltage, R is a load resistance, S is a switch, and D is a diode. In the periodic steady-state, the mean voltage $\bar{v}$ and mean current $\bar{i}$ are given by

$$\begin{pmatrix} \bar{i} \\ \bar{v} \end{pmatrix} = \begin{pmatrix} \dfrac{1}{R(1-d)^2} \\ \dfrac{1}{1-d} \end{pmatrix} V_{\mathrm{PV}}, \tag{1}$$

where R is the load resistance, and d is the duty cycle of the boost converter. Equation (1) indicates that the output power of the PV system is a function of the duty cycle d. Hence, the PV system modulates the duty cycle to find the global MPP. As a result, an MPPT control problem can be characterized as a one-dimensional black-box optimization problem, where the objective function is the output of the PV array, and the decision variable is the duty cycle of the converter.

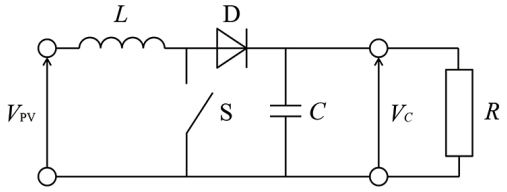

FIGURE 4. Boost converter

Meanwhile, in addition to the P-V curves, the power-duty (P-D) curves also exhibit multiple local MPPs, as shown in Figure 3(c). In these cases, typical MPPT methods may find local MPPs. To make the most of solar power, an MPPT control algorithm, which aims to obtain the global MPP, is required.

3. Bayesian Optimization.

BO addresses the following optimization problem:

$$\max_{x \in \mathcal{X}} f(x), \tag{2}$$

where $f : \mathcal{X} \to \mathbb{R}$ is a black-box function, and $\mathcal{X} \subset \mathbb{R}$ is a closed interval.

Remark 3.1. *As described in the previous section, since the MPPT control problem is a one-dimensional optimization problem, we suppose $f : \mathcal{X} \to \mathbb{R}$ in this paper.*

At iteration $n \in \mathbb{N}$, suppose that we observe

$$y_n = f(x_n) + \epsilon_n, \tag{3}$$

where ϵ_n is noise which follows a Gaussian distribution with zero mean and variance σ^2 (i.e., $\epsilon_n \sim \mathcal{N}(0, \sigma^2)$).

BO is performed by repeating the following process:

- Express the prior information on f as a statistical model P;
- Choose a next observation point x_n based on P;
- Observe the corresponding function value y_n;
- Update P based on $\mathcal{D}_{1:n} = \{(x_1, y_1), \ldots, (x_n, y_n)\}$.

We introduce a Gaussian process (GP) to express the statistical model P.

This section first explains some mathematical preliminaries. Next, we describe the BO algorithm.

3.1. Mathematical preliminaries.

3.1.1. *Gaussian process.* The GP is formally defined as follows [16].

Definition 3.1. *The GP is a collection of random variables, any finite number of which have (consistent) joint Gaussian distributions.*

The function f follows the GP if for any $x_1, \ldots, x_n \in \mathcal{X}$, the vector $\boldsymbol{f}_{1:n} = [f(x_1) \cdots f(x_n)]^T$ follows the n-dimensional Gaussian distribution with mean

$$\boldsymbol{m}_{1:n} = [\mu(x_1) \cdots \mu(x_n)]^T \tag{4}$$

and covariance matrix

$$\Sigma_{1:n} = \begin{bmatrix} k(x_1, x_1) & \cdots & k(x_1, x_n) \\ \vdots & \ddots & \vdots \\ k(x_n, x_1) & \cdots & k(x_n, x_n) \end{bmatrix}, \tag{5}$$

where $\mu : \mathcal{X} \to \mathbb{R}$ and $k : \mathcal{X} \times \mathcal{X} \to \mathbb{R}^+$ are the mean function and the kernel function, respectively. For convenience, we assume that $\mu(x) = 0$ in this study. The GP can be characterized by its mean function μ and kernel function k. In this study, we use a Matérn 5/2 kernel [15] as the kernel function k:

$$k^{\mathrm{M5/2}}(x, x') = \theta \left(1 + \sqrt{5r^2(x, x')} + \frac{5}{3} r^2(x, x')\right) \cdot \exp\left(-\sqrt{5r^2(x, x')}\right), \tag{6}$$

where θ is a parameter, and

$$r^2(x, x') = (x - x')^2. \tag{7}$$

Remark 3.2. *In GP, 5/2 or 3/2 is often chosen as the parameter because BO with these parameters has good empirical optimization performance and is also suitable for theoretical analysis. In MPPT control, 5/2 is chosen to take account of the characteristics of the PV panel* [15].

3.1.2. *Posterior distribution.* In BO, we calculate the posterior distribution of $f(x_{n+1})$ by using the past observation points $\mathcal{D}_{1:n}$. The joint distribution of $\boldsymbol{f}_{1:n}$ and $f(x_{n+1})$ is as follows [17]:

$$\begin{bmatrix} \boldsymbol{f}_{1:n} \\ f(x_{n+1}) \end{bmatrix} \sim \mathcal{N}\left(\boldsymbol{0}, \begin{bmatrix} \Sigma_{1:n} + \sigma^2 I_n & \boldsymbol{k}_{1:n}(x_{n+1}) \\ \boldsymbol{k}_{1:n}(x_{n+1})^T & k(x_{n+1}, x_{n+1}) \end{bmatrix}\right), \tag{8}$$

where I_n is the n-dimensional identity matrix, and $\boldsymbol{k}_{1:n}(x_{n+1})$ is the vector $[k(x_{n+1}, x_1) \cdots k(x_{n+1}, x_n)]^T$. By using this relationship, we have the posterior distribution of $f(x_{n+1})$ (i.e., conditional probability distribution of $f(x_{n+1})$ given $\boldsymbol{y}_{1:n} = [y_1 \cdots y_n]^T$) as follows [17]:

$$p(f(x_{n+1}) | \boldsymbol{f}_{1:n}, x_{n+1}) = \mathcal{N}\left(\mu_n(x_{n+1}), \sigma_n^2(x_{n+1})\right), \tag{9}$$

where

$$\mu_n(x_{n+1}) = \boldsymbol{k}_{1:n}(x_{n+1})^T \left(\Sigma_{1:n} + \sigma^2 I_n\right)^{-1} \boldsymbol{y}_{1:n}, \tag{10}$$

$$\sigma_n^2(x_{n+1}) = k(x_{n+1}, x_{n+1}) - \boldsymbol{k}_{1:n}(x_{n+1})^T \left(\Sigma_{1:n} + \sigma^2 I_n\right)^{-1} \boldsymbol{k}_{1:n}(x_{n+1}). \tag{11}$$

3.2. **BO algorithm.** BO uses an alternative function a based on the probability distribution of $f(x_{n+1})$ and chooses a next observation point as follows:

$$x_{n+1} = \arg\max_{x \in \mathcal{X}} a(x). \tag{12}$$

This alternative function is called an acquisition function. The acquisition function depends on the kernel function k and the past observation points $\mathcal{D}_{1:n}$.

Many acquisition functions have been proposed, such as maximum probability of improvement and expected improvement [18]. In this paper, we use the well-known upper confidence bound (UCB) scheme [18], which is a simple and intuitive form as follows:

$$a^{\mathrm{UCB}}(x) = \mu_n(x) + \beta \sigma_n^2(x), \tag{13}$$

where the parameter β controls the trade-off between exploration and exploitation.

From Subsection 3.1, the procedure of BO consists of three steps as follows:

- Derive the posterior distribution of $f(x_{n+1})$ based on k and $\mathcal{D}_{1:n}$;
- Choose a next observation point x_{n+1} based on an acquisition function;
- Observe y_{n+1}.

The pseudocode of BO is presented in Algorithm 1.

Algorithm 1. Bayesian optimization

Input: Max iteration N, $n = 1$, and initial input x_1.
Observe y_1 via (3).
while $n \leq N$ **do**
  Calculate μ_{n+1} and σ^2_{n+1} via (10) and (11).
  Calculate x_{n+1} via (12).
  Observe y_{n+1} via (3).
  Add (x_{n+1}, y_{n+1}) to $\mathcal{D}_{1:n+1}$.
  Increment n.
end while
Output: $x_{i^\star}$, where $i^\star \in \arg\max_{i=1,\ldots,N} y_i$.

4. **Modified Bayesian Optimization.** This paper presents MBO which utilizes the gradient information, i.e., the Lipschitz constant of the objective function. The presented algorithm improves the performance of standard BO by restricting the region where the optimal solution does not exist.

4.1. **Lipschitz condition.** In this study, to utilize the Lipschitz continuity of the objective function, we add the following assumption.

Assumption 4.1. *The objective function f satisfies the Lipschitz condition with a Lipschitz constant $K > 0$:*

$$|f(\alpha) - f(\beta)| \leq K|\alpha - \beta| \qquad \forall \alpha, \beta \in \mathcal{X}. \tag{14}$$

In other words, the absolute value of the rate of change of f is at most K:

$$K \geq \max_{\alpha \neq \beta} \left| \frac{f(\alpha) - f(\beta)}{\alpha - \beta} \right|. \tag{15}$$

We now construct the zigzag function with gradient $\pm K$ by using the Lipschitz constant K, as shown in Figure 5. From the Lipschitz condition (14), we have

$$f(x_i) - K|x - x_i| \leq f(x) \leq f(x_i) + K|x - x_i| \qquad \forall x, x_i \in \mathcal{X}, \tag{16}$$

which means that the objective function exists in the parallelogram regions in Figure 5. For explanation of the presented algorithm, we define the following notation:

$$\bar{\mathcal{D}}_{1:n} = \{(\bar{x}_1, \bar{y}_1), \ldots, (\bar{x}_n, \bar{y}_n)\}.$$

The set $\bar{\mathcal{D}}_{1:n}$ is the set sorted in ascending order with respect to the x-coordinate of $\mathcal{D}_{1:n}$. We also define $\left(\bar{x}_i^{\mathrm{U}}, \bar{y}_i^{\mathrm{U}}\right)$ as the upper vertices of the parallelogram in Figure 5, where

$$\begin{cases} \bar{x}_i^{\mathrm{U}} = \dfrac{K(\bar{x}_i + \bar{x}_{i+1}) + \bar{y}_{i+1} - \bar{y}_i}{2K} \\ \bar{y}_i^{\mathrm{U}} = \dfrac{K(\bar{x}_{i+1} - \bar{x}_i) + \bar{y}_i + \bar{y}_{i+1}}{2} \end{cases} \tag{17}$$

for all $i \in \{1, \ldots, n-1\}$.

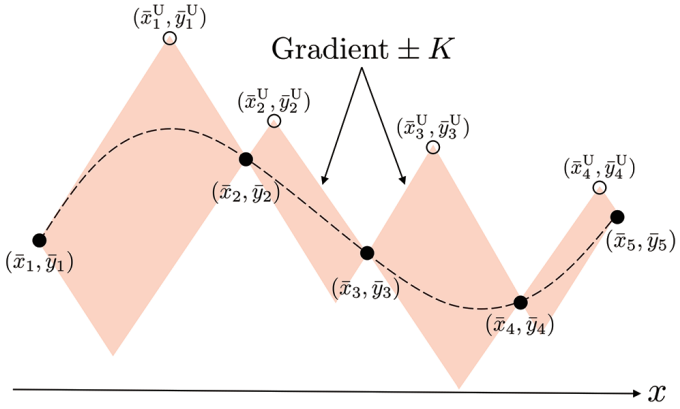

FIGURE 5. Graphical interpretation of Lipschitz condition

4.2. **Modified Bayesian optimization algorithm.** We attempt to introduce the Lipschitz continuity of the objective function into the standard BO algorithm. As we described in the previous section, at each iteration of the standard BO algorithm, the mean function μ_n and the covariance function σ_n^2 are calculated. At the same time, MBO constructs the lines with gradient $\pm K$ from the past observation points, as shown in Figure 6. Now, let us define

$$\mathcal{J}_{n+1} = \left\{ j \in \{1, \ldots, n-1\} \,\middle|\, \max_{i=1,\ldots,n} y_i > \bar{y}_j^{\mathrm{U}} \right\}. \tag{18}$$

Then, the global optimal solution does not exist in the interval $[\bar{x}_k, \bar{x}_{k+1}]$ for all $k \in \mathcal{J}_{n+1}$ because of the Lipschitz continuity of the objective function. MBO rejects such interval $[\bar{x}_k, \bar{x}_{k+1}]$ from the domain of the acquisition function a and reduces unnecessary exploration, as shown in Figure 6. As a result, MBO accelerates the convergence of BO. Moreover, it is noteworthy that the MBO algorithm does not terminate later than the standard BO algorithm at worst.

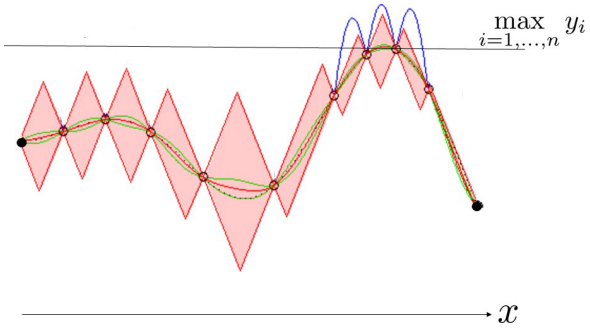

FIGURE 6. Operating principle of MBO

The pseudocode of the MBO algorithm is summarized in Algorithm 2, where

$$\hat{a}(x) = \begin{cases} -\infty & \text{if } \bar{x}_k \le x \le \bar{x}_{k+1} \quad \forall k \in \mathcal{J}_{n+1} \\ a(x) & \text{otherwise,} \end{cases} \tag{19}$$

$$x_{n+1} = \arg\max_{x \in \mathcal{X}} \hat{a}(x). \tag{20}$$

Algorithm 2. Modified Bayesian optimization

1: **Input:** Max iteration N, $n = 1$, and initial input x_1.
2: Observe y_1 via (3).
3: **while** $n \leq N$ **do**
4: Calculate μ_{n+1} and σ^2_{n+1} via (10) and (11).
5: Calculate the upper vertices $\left(\bar{x}_i^{\mathrm{U}}, \bar{y}_i^{\mathrm{U}}\right)$ via (17).
6: Calculate $\mathcal{J}_{n+1}$ via (18).
7: Calculate $\hat{a}$ via (19).
8: Calculate x_{n+1} via (20).
9: Observe y_{n+1} via (3).
10: Add (x_{n+1}, y_{n+1}) to $\mathcal{D}_{1:n+1}$.
11: Increment n.
12: **end while**
13: **Output:** $x_{i^\star}$, where $i^\star \in \arg\max_{i=1,\ldots,N} y_i$.

Remark 4.1. *It is noteworthy that the different processes between BO and MBO (i.e., fifth and sixth lines of Algorithm 2) are computationally inexpensive because only linear functions and their intersections are calculated.*

5. **Simulation.** In this section, we first describe the simulation model and the parameters of the PV system. Next, we explain the prior simulations required to apply MBO to the MPPT control problem. Finally, we show the simulation results and compare MBO with LO [10] and standard BO [15]-based MPPT methods.

5.1. **Simulation model.** All the simulations were performed using Simscape Electrical from MATLAB/Simulink on a computer with an Intel Core i7-7700K CPU 4.20 GHz processor having 32 GB of RAM in a Windows 10 environment. The sampling time of the simulation was taken as 0.1 ms. The calculated duty cycle via MPPT algorithms was updated every $t_{\mathrm{duty}} = 0.2$ s and was set in the range of $[0.1, 0.9]$ [10]. The circuit parameters of the boost converter were listed in Table 1. The resistive load was $R = 10\ \Omega$. The 1STH-215-P PV array model prepared in Simscape Electrical was used in this study. To simulate the P-V curves with multiple local MPPs, the three PV array models were connected in series. The panel temperature was constant at 25°C. The simulation time was $t_{\mathrm{sim}} = 10$ s.

Table 1. Circuit parameters of boost converter

Parameter	Value
L	0.1 H
C	10^{-3} μF
Switching frequency	20 kHz

5.2. **Prior simulation.** To apply MBO to the MPPT control problem, we preliminarily determined the parameter K based on the gradients of the P-D curves. Four irradiance conditions for determining the relevant parameter K are listed in Table 2, where G_1, G_2, and G_3 express the amounts of solar radiation for each of the three PV array models. In Figures 7 and 8, the corresponding P-D curves and their absolute values of gradients are illustrated. Table 3 shows the smallest Lipschitz constant $K^\star$ in each case. Since the P-D characteristics depend on the irradiance conditions, the Lipschitz constants also

depend on the P-D characteristics. Thus, the Lipschitz constants depend on the irradiance conditions. In this study, the parameter of LO and MBO was determined as $K = 1000$ based on Table 3 to subsume all the irradiance conditions.

TABLE 2. Irradiance conditions for determining K

Case	G_1 (W/m^2)	G_2 (W/m^2)	G_3 (W/m^2)
1	1000	1000	1000
2	1000	800	800
3	800	600	400
4	1000	800	600

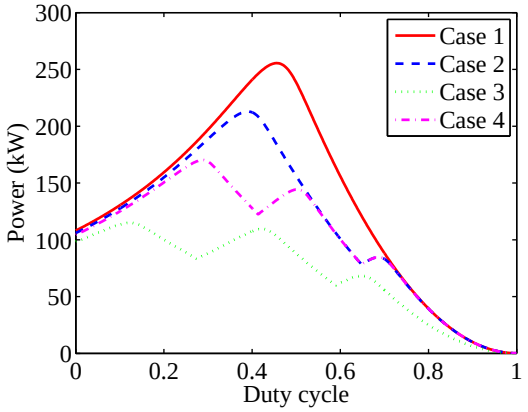

FIGURE 7. P-D curves under conditions of Table 2

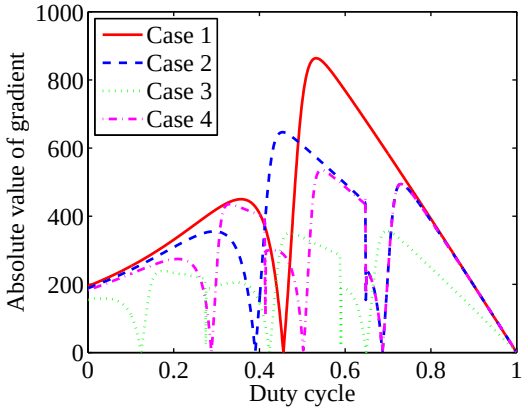

FIGURE 8. Absolute values of gradients of P-D curves

TABLE 3. Smallest Lipschitz constant $K^\star$

Case	$K^\star$
1	864
2	647
3	356
4	536

5.3. **Simulation results.** In this subsection, we compare the presented MBO with LO and BO in terms of power loss. The power loss is defined as follows:

$$W_{\text{loss}} = \sum_{n=1}^{n_{\text{sim}}} (P^\star - P_n)\, t_{\text{duty}}, \tag{21}$$

where n_{sim} is the number of iterations in the simulation (i.e., $n_{\text{sim}} = t_{\text{sim}}/t_{\text{duty}} = 50$), $P^\star$ is the maximum power, and P_n is the output power at iteration n. We randomly sampled ten irradiance conditions from a uniform distribution over $[100, 1000]$, as listed in Table 4.

TABLE 4. Ten irradiance conditions for verification

Case	G_1 (W/m^2)	G_2 (W/m^2)	G_3 (W/m^2)
1	490	350	780
2	440	710	330
3	790	690	560
4	820	240	730
5	270	200	910
6	540	550	970
7	500	970	590
8	680	400	220
9	740	630	230
10	780	300	330

Figures 9 and 10 illustrate the duty cycle and power, respectively, of Case 4 as typical results. In this case, the global MPP is $x^\star = 0.48$. We can see from these figures that LO finds the global MPP but it explores power points far from the global MPP around 5 s and 9 s. BO also finds the global MPP but it explores the many low power points between 2 s and 4 s. On the other hand, MBO finds the global MPP faster than LO and BO. This is due to the fact that the candidate regions containing the global MPP are restricted by LO, as described in Subsection 4.2. Figure 11 illustrates the comparison of the losses of the MPPT methods for ten randomly sampled irradiance cases. We can see from Figure 11 that the loss of MBO is the lowest in all the cases.

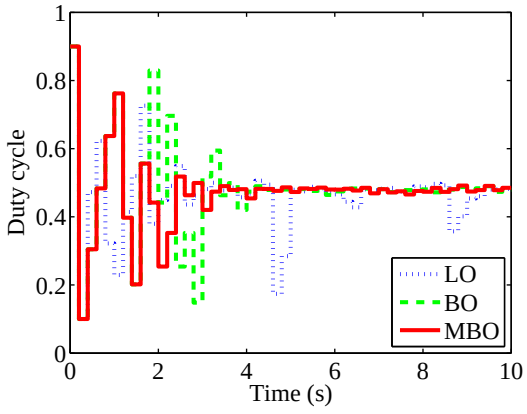

FIGURE 9. Duty cycles of MPPT methods

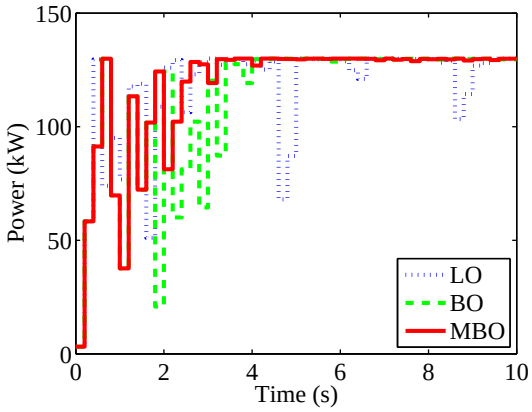

FIGURE 10. Power of MPPT methods

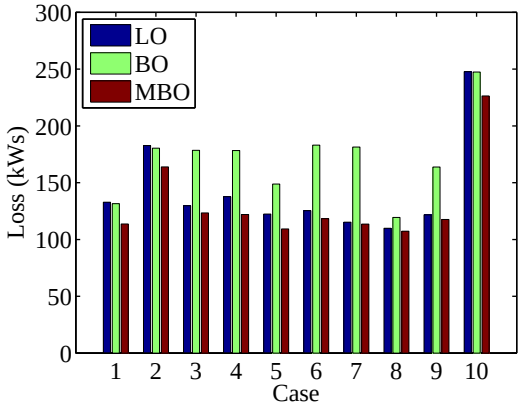

FIGURE 11. Power loss of MPPT methods

6. **Conclusions.** In this paper, we presented MBO and applied it to the MPPT control problem. By utilizing the Lipschitz continuity of the objective function, the presented algorithm improved the convergence performance. The effectiveness of MBO was verified through simulations. Simulation results showed that the presented MBO algorithm finds the global MPP faster than the standard BO algorithm.

REFERENCES

[1] E. Koutroulis, K. Kalaitzakis and N. C. Voulgaris, Development of a microcontroller-based, photovoltaic maximum power point tracking control system, *IEEE Transactions on Power Electronics*, vol.16, no.1, pp.46-54, 2001.

[2] Y.-C. Kuo, T.-J. Liang and J.-F. Chen, Novel maximum-power-point-tracking controller for photovoltaic energy conversion system, *IEEE Transactions on Industrial Electronics*, vol.48, no.3, pp.594-601, 2001.

[3] A. A. Ghassami, S. M. Sadeghzadeh and A. Soleimani, A high performance maximum power point tracker for PV systems, *International Journal of Electrical Power & Energy Systems*, vol.53, pp.237-243, 2013.

[4] K. El Hammoumi, R. Chaibi and R. El Bachtiri, Fuzzy state-feedback control for MPPT of photovoltaic energy with storage system, *International Journal of Innovative Computing, Information and Control*, vol.18, no.1, pp.253-270, 2022.

[5] F. A. Samman, T. Suhaebri, R. S. Sadjad, A. E. U. Salam, A. Achmad and C. Machbub, MPPT algorithm using decremented window-scanning method for home scale photovoltaic-based power supply systems, *International Journal of Innovative Computing, Information and Control*, vol.17, no.2, pp.527-538, 2021.

[6] S. Mohanty, B. Subudhi and P. K. Ray, A new MPPT design using grey wolf optimization technique for photovoltaic system under partial shading conditions, *IEEE Transactions on Sustainable Energy*, vol.7, no.1, pp.181-188, 2016.
[7] C. Huang, L. Wang, R. S.-C. Yeung, Z. Zhang, H. S.-H. Chung and A. Bensoussan, A prediction model-guided Jaya algorithm for the PV system maximum power point tracking, *IEEE Transactions on Sustainable Energy*, vol.9, no.1, pp.45-55, 2018.
[8] H. Deboucha, S. Mekhilef, S. Belaid and A. Guichi, Modified deterministic Jaya (DM-Jaya)-based MPPT algorithm under partially shaded conditions for PV system, *IET Power Electronics*, vol.13, no.19, pp.4625-4632, 2020.
[9] B. Yang, L. Zhong, X. Zhang, H. Shu, T. Yu, H. Li, L. Jiang and L. Sun, Novel bio-inspired memetic salp swarm algorithm and application to MPPT for PV systems considering partial shading condition, *Journal of Cleaner Production*, vol.215, pp.1203-1222, 2019.
[10] W. Li, G. Zhang, T. Pan, Z. Zhang, Y. Geng and J. Wang, A Lipschitz optimization-based MPPT algorithm for photovoltaic system under partial shading condition, *IEEE Access*, vol.7, pp.126323-126333, 2019.
[11] S. A. Piyavskii, An algorithm for finding the absolute extremum of a function, *USSR Computational Mathematics and Mathematical Physics*, vol.12, no.4, pp.57-67, 1972.
[12] B. O. Shubert, A sequential method seeking the global maximum of a function, *SIAM Journal on Numerical Analysis*, vol.9, no.3, pp.379-388, 1972.
[13] E. Masuda, Y. Wakasa and R. Adachi, Adaptive Piyavskii-Shubert algorithm and its application to maximum power point tracking control, *Journal of Control, Automation and Electrical Systems*, vol.33, no.4, pp.1342-1353, 2022.
[14] E. Masuda, Y. Wakasa and R. Adachi, Modified Lipschitz optimization and its application to maximum power point tracking control for photovoltaic systems, *IEEJ Transactions on Electrical and Electronic Engineering*, vol.17, no.6, pp.816-822, 2022.
[15] H. Abdelrahman, F. Berkenkamp, J. Poland and A. Krause, Bayesian optimization for maximum power point tracking in photovoltaic power plants, *Proc. of the 2016 European Control Conference*, pp.2078-2083, 2016.
[16] C. E. Rasmussen, *Gaussian Processes in Machine Learning*, Springer, 2004.
[17] C. E. Rasmussen and C. K. I. Williams, *Gaussian Processes for Machine Learning*, MIT Press, 2006.
[18] J. Snoek, H. Larochelle and R. P. Adams, Practical Bayesian optimization of machine learning algorithms, *Advances in Neural Information Processing Systems 25*, pp.2960-2968, 2012.

Author Biography

Eiji Masuda received his B.S. and M.S. degrees from Yamaguchi University, Japan, in 2019 and 2021, respectively. Since April 2021, he has been working with Yamaguchi Prefectural Industrial Technology Institute. His research interests include application of optimization theory to power systems. He is a member of SICE.

Yasuki Sogawa received his B.S. degree from Yamaguchi University, Japan, in 2021. Since April 2021, he has been working with Chudenko Corporation. He is currently engaged in construction management of electrical work. His research interests include application of optimization theory to power systems.

Yuji Wakasa received the B.S. and M.S. degrees in Engineering and the degree of Doctor of Informatics all from Kyoto University, Japan, in 1992, 1994, and 2000, respectively. He was a Research Associate at Okayama University from 1994 to 1998 and at Kyoto University from 1998 to 2002. Since October 2002, he has been with Yamaguchi University, where he is currently a Professor. His current research interests include control system design via mathematical programming and its applications. He is a member of SICE, ISCIE, IEEJ, and IEEE.

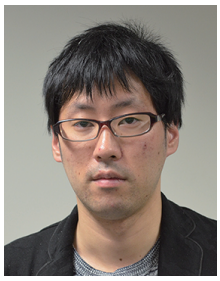

Ryosuke Adachi received his B.E., M.S.I., and Ph.D. degrees from Hokkaido University, Japan, in 2014, 2016, and 2019, respectively. Since 2019, he has been an Assistant Professor at the Graduate School of Sciences and Technology for Innovation at Yamaguchi University. His research interests include the estimation of distributed control systems. He is a member of SICE, ISCIE and IEEE.